FIGURES

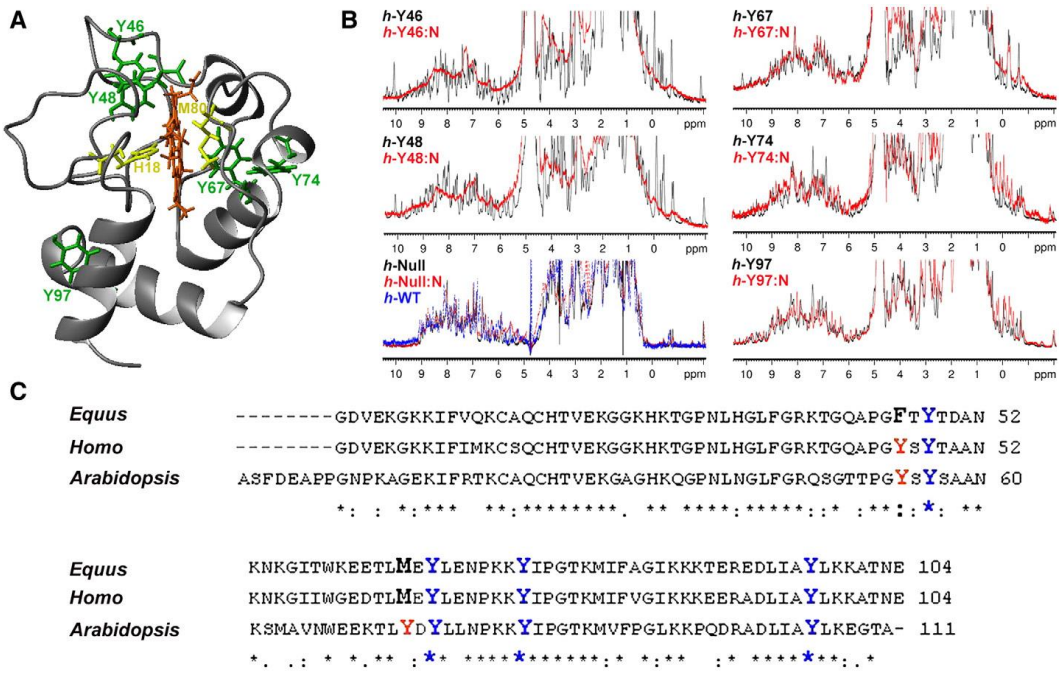

Fig. 1. Structural features of Cc. (A) Ribbon representation of the solution NMR structure of human Cc (PDB code 1J3S). The five tyrosine residues are in green, the haem group is in orange, and the two axial ligands are in yellow. (B) 1D NMR spectra of the five oxidised monotyrosine mutants of human Cc in their non-nitrated or nitrated state. Each of the socalled h-Y46, h-Y48, h-Y67, h-Y74 and h-Y97 Cc mutants has all its tyrosine residues but one (just that giving its number to the mutant) replaced by phenylalanines. 1D NMR spectra of the wild-type form (h-WT) and of the mutant having all five tyrosines replaced by phenylalanines (h-Null) are also shown for comparative purposes. As a control, the 1D NMR spectrum of the h-Null mutant submitted to the nitration process (h-Null:N) is presented. (C) Amino acid sequence alignment of horse (Equus), human (Homo) and plant (Arabidopsis) Cc. Horse Cc contains four tyrosines, human Cc has five tyrosines, and plant Cc has six tyrosines. The four common tyrosine residues are coloured in blue, whereas the non-conserved tyrosines are in red.

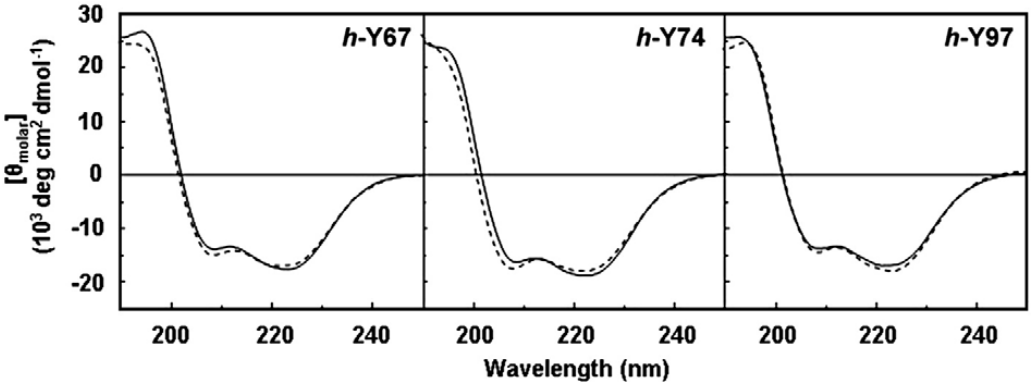

Fig. 2. Effect of nitration on the secondary structure of oxidised Cc mutants. Far-UV CD spectra of both the non-nitrated (solid line) and nitrated (dashed line) forms of h-Y67, h-Y74 and h-Y97 were recorded. Samples were prepared as described under Materials and methods.

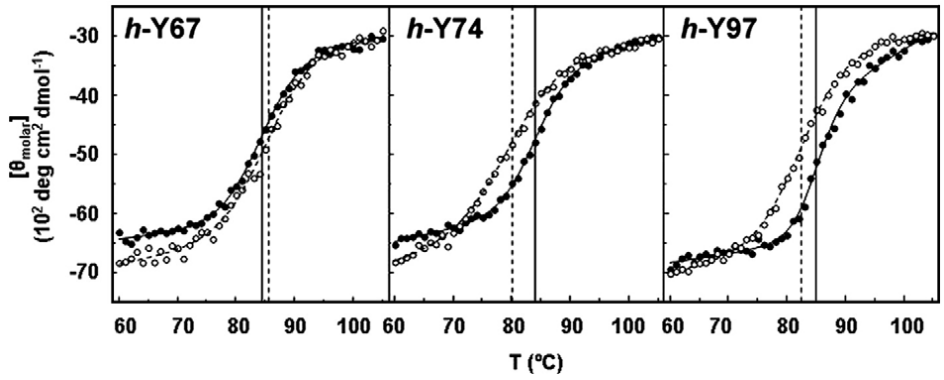

Fig. 3. Effect of nitration on the thermal stability of oxidised Cc mutants. The changes in the 220 nm CD signal of both the non-nitrated (black circles) and nitrated (white circles) forms of h-Y67, h-Y74 and h-Y97 were determined at varying temperatures. Fitted curves are shown by solid or dashed lines for the non-nitrated and nitrated species, respectively. The resulting values for midpoint melting temperature (T_m) are indicated by vertical lines, which are likewise solid or dashed for the non-nitrated or nitrated species, respectively.

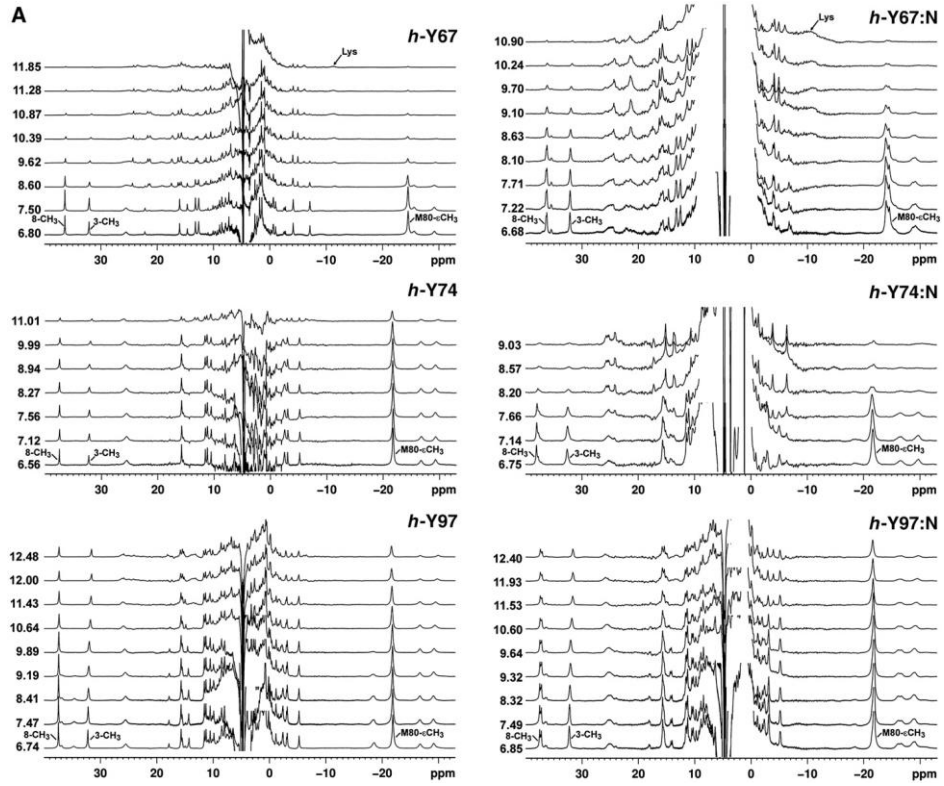

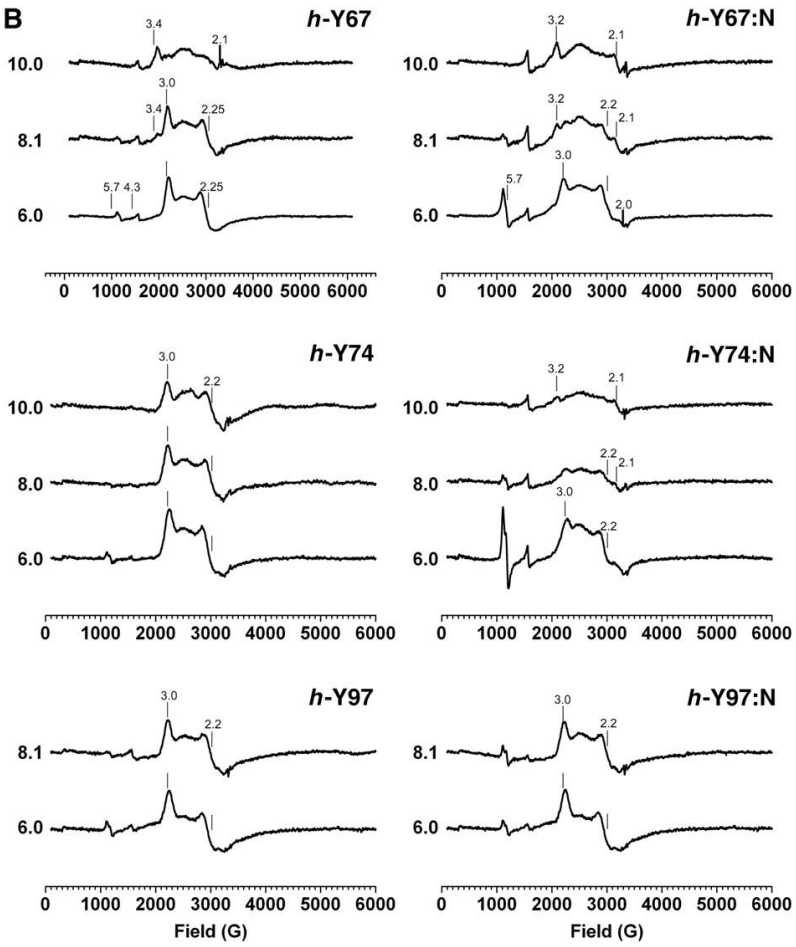

Fig. 4. pH titrations of oxidised Cc mutants by NMR and EPR spectroscopies. (A) The SuperWEFT 1D ^{1}H NMR spectra showing the paramagnetic region of the non-nitrated and nitrated forms of h-Y67, h-Y74 and h-Y97 were recorded at varying pH values, which are those marked on the left of each spectrum. The resonances of the haem methyl groups and the Met80 methyl signals are highlighted in the spectrum recorded at the starting point of the titration. The arrows point to the signal of lysine, which replaces Met80 as an Fe axial ligand in the alkaline Cc species. The alkaline transition pK_a value for each monotyrosine mutant is calculated by fitting the volume of the labelled NMR signals to the Henderson-Hasselbalch function, as summarised in Table 2. Reversibility is corroborated for all mutants – nitrated and non-nitrated – by recording the last 1D ^{1}H NMR spectrum at the initial pH value (data not shown). (B) EPR spectra of the non-nitrated and nitrated forms of h-Y67, h-Y74 and h-Y97 were recorded at varying pH values, which are those marked on the left of each spectrum. The g-values (g_z and g_y) of the main signals are also marked. A background spectrum of the sample buffer has been subtracted and the baseline has been corrected using a 3rd power polynomial.

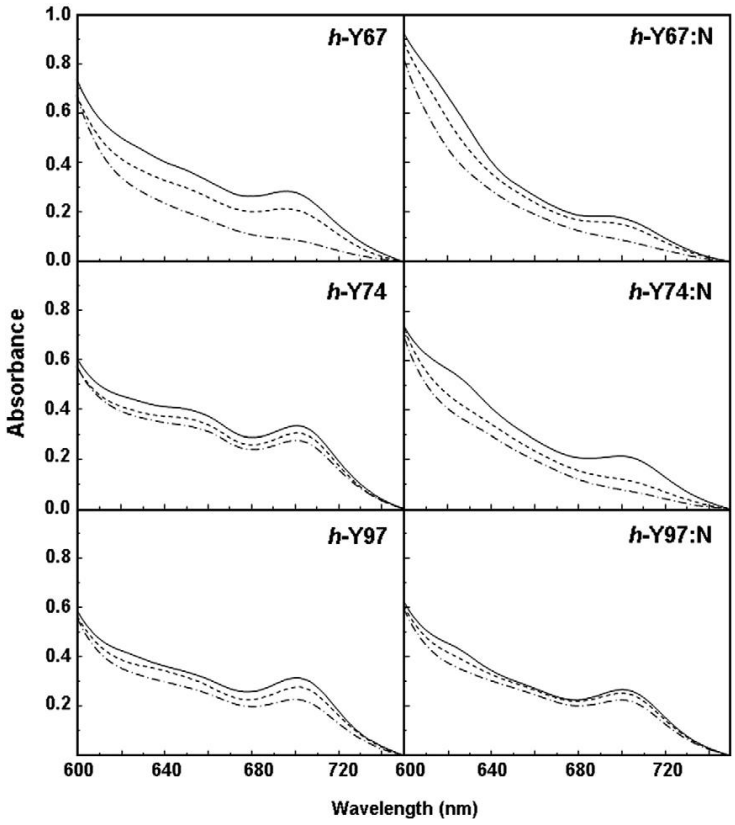

Fig. 5. pH titrations of oxidised Cc mutants by following the electronic absorption band at 699 nm. Electronic absorption spectra of the non-nitrated and nitrated forms of h-Y67, h-Y74 and h-Y97 were recorded at three pH values, namely pH 6.7 (solid line), pH 8.0 (dashed line) and pH 9.6 (dash-dotted line). The full set of data was fitted to the Henderson-Hasselbalch equation to calculate the pK_a value for each monotyrosine mutant, as summarised in Table 2.

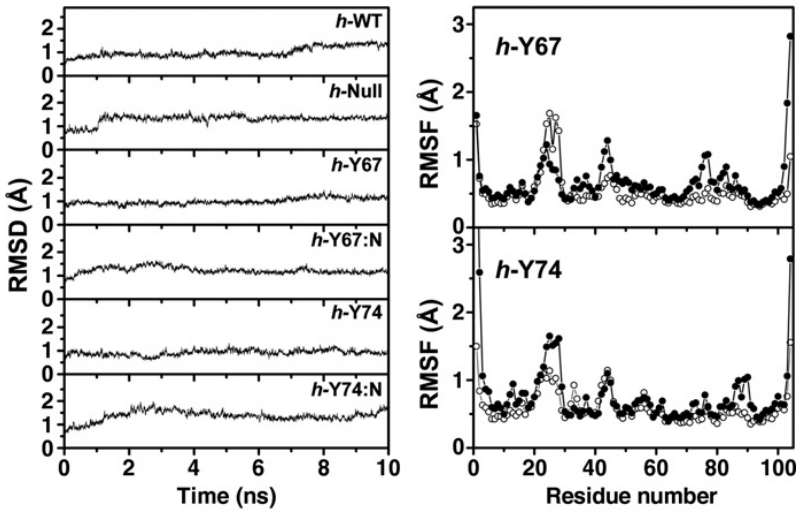

Fig. 6. Molecular dynamics calculations of oxidised Cc species. (Left) Root mean square deviation (RMSD) of backbone atoms from snapshots taken every 4 ps from the MD trajectories. (Right) , Comparisons of backbone atomic fluctuations, in a per residue basis, of the different trajectories. Root mean square fluctuations (RMSF) were calculated after aligning the backbone atoms of each snapshot to the average structure of the production run. RMSF per residue of h-Y67 and h-Y74 is represented by open circles, whereas that of h-Y67:N and h-Y74:N is represented by solid circles.

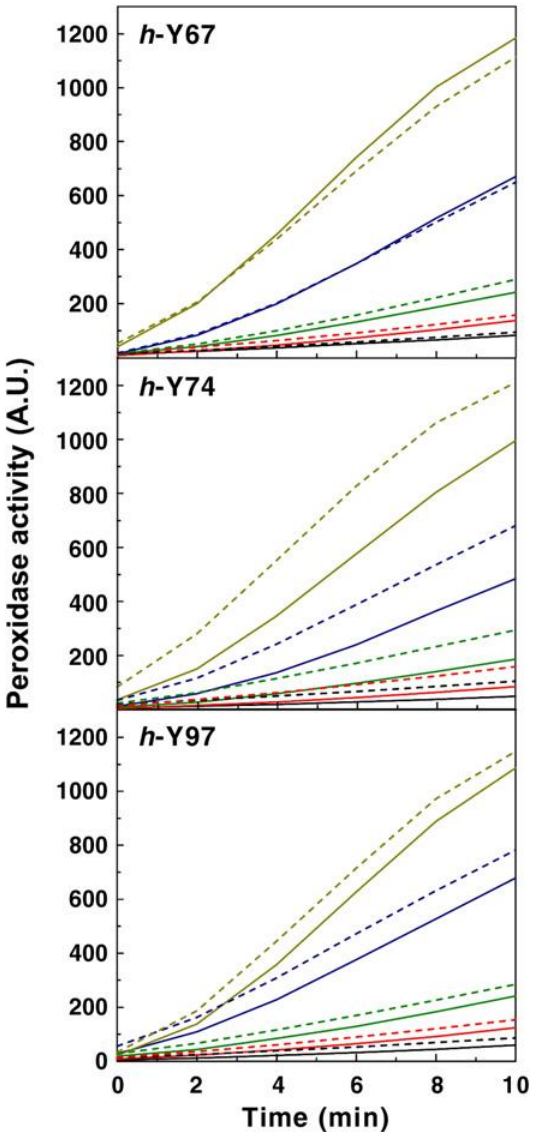

Fig. 7. In vitro peroxidase activity of oxidised Cc mutants. The peroxidase activity of the nitrated (dashed lines) and non-nitrated (solid lines) forms of h-Y67, h-Y74, h-Y97 was measured by following the increase in fluorescence because of 2'7'-dichlorofluorescein (H_2DCF) oxidation. BSA was used as a control. Results are the average of at least eight independent measurements. The pH values were: 7.0 (black), 7.5 (red), 8.0 (green), 8.5 (dark blue) and 9.0 (dark yellow).

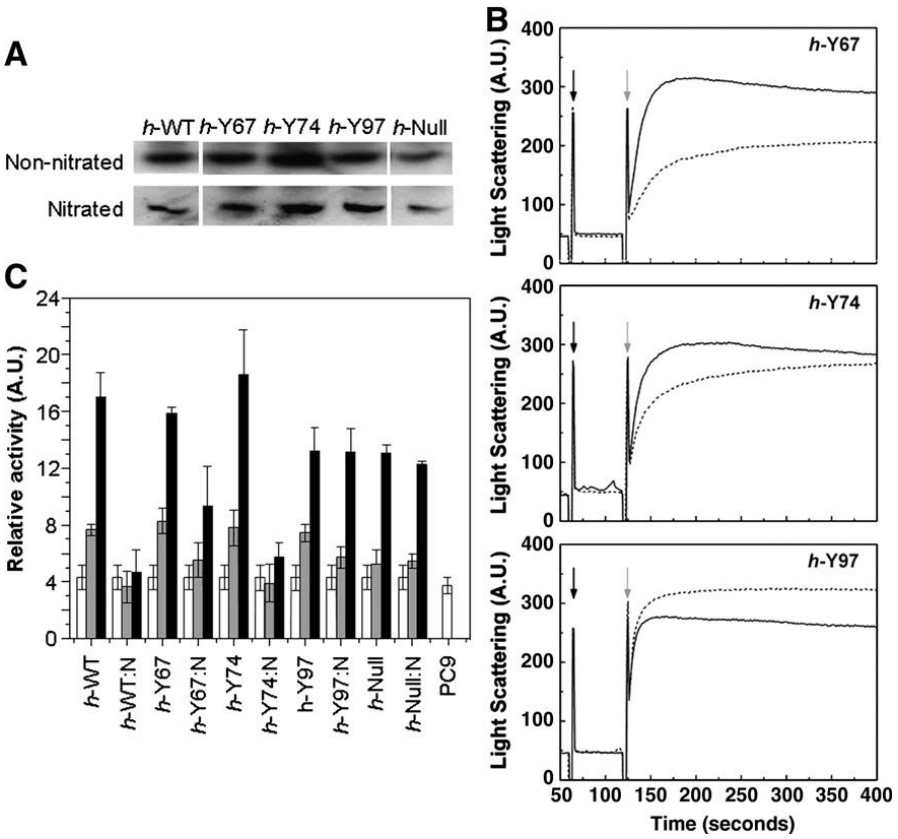

Fig. 8. Interaction between Apaf-1 and Cc species. (A) Cross-linking between Apaf-1 and the non-nitrated or nitrated Cc species, as detected by Western blot using antibodies against Cc. (B) Complex formation of Apaf-1 with non-nitrated (solid lines) and nitrated (dashed lines) Cc mutants, as determined by light scattering. The arrows indicate when Apaf-1 (in black) and Cc (in grey) were added to the buffer solution. (C) Activation of caspase-9 as determined by following the increase in fluorescence after substrate (Ac-LEHD-AFC) cleavage by means of the incubation of Apaf-1 and PC9 with both nitrated and non-nitrated Cc species. Cc concentrations were: 0 (white), 20 nM (grey) and 40 nM (black).

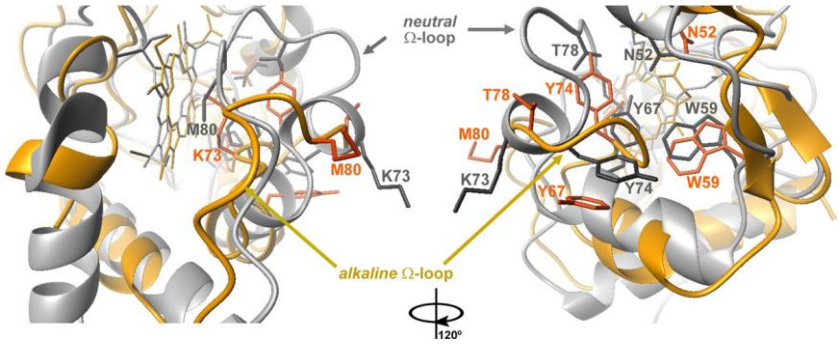

Fig. 9. Superposition of the structures of 'neutral' human Cc and 'alkaline' yeast Cc. Ribbon representation of human Cc (PDB code 1J3S; [40]) is displayed in grey, whereas that of 'alkaline' yeast iso-1-cytochrome is coloured in yellow (PDB code 1LMS; [22]). The Ω-loop for each structure, along with those residues involved in the contacts network described in the text, are labelled following the same colour-code. Noteworthy, the Met80 is substituted by Lys73 in the 'alkaline' structure in which Lys72 and Lys79 were mutated by alanine residues. A two-antiparallel-β-strand hairpin is highlighted in the yeast structure. The picture was prepared using the MOLMOL program [72].

TABLES

Table 1
Midpoint melting temperature (Tm) of WT and mutant Cc, in their non-nitrated and nitrated states, as calculated by CD and DS.

	Non-nitrated	Nitrated

	CD	DSF	CD	DSF
h-WT	85.9±0.2	81.8±1.9	n.d.[a]	n.d[a]
h-Y67	84.5±0.3	81.9±1.4.	85.7±0.8	82.7±0.5
h-Y74	84.0±0.2	81.9±1.5	80.1±0.5	76.0±2.6
h-Y97	85.0±0.3	84.3±1.6	82.5±0.3	81.3±1.3
h-Null	85.3±0.2	83.9±2.0	85.0±0.5[b]	83.8±2.1[b]

[a] n.d., not determined, because polynitrated WT Cc was a non-homogeneous sample.
[b] The h-Null mutant was submitted to the same nitration protocol as the other Cc species, as a control.

Table 2
Alkaline transition pK_a of WT and Cc mutants, in their non-nitrated and nitrated states, as determined by optical and NMR spectroscopies.

	A699 nm titration		NMR titration	
	Non-nitrated	**Nitrated**	**Non-nitrated**	**Nitrated**
h-WT	9.5±0.2	n.d.[a]	9.3±0.1	n.d.[a]
h-Y67	8.8±0.6	8.3±0.2	8.5±0.2	8.3±0.3
h-Y74	11.3±0.3	7.8±0.1	≥ 10.0	7.8±0.1
h-Y97	≥ 12	11±0.3	≥ 11.0	≥ 11.0
h-Null	11.6±0.9	11.6±1.6[b]	≥ 10.0	≥ 10.0[b]

[a] n.d., not determined, because polynitrated WT Cc was a non-homogeneous sample.
[b] The h-Null mutant was submitted to the same nitration protocol as the other Cc species, as a control.